

Covariance matrices for ENDF/B-VII $^{235,238}\text{U}$ and ^{239}Pu evaluated files in the fast energy range

P. Talou^{1,2}, T. Kawano¹, and P.G. Young¹

¹ T-16, Nuclear Physics, Los Alamos National Laboratory, USA

² DEN/DER/SPRC/Laboratoire d'Études de Physique, CEA, France

Abstract. Covariance matrices for evaluated ENDF/B-VII files of $^{235,238}\text{U}$ and ^{239}Pu are obtained in the fast energy region. Both differential experimental data and theoretical model calculations are used to estimate the uncertainties and correlations associated with the evaluated cross sections. The results are compiled in the ENDF format for covariance matrices, and processed into multi-group files for applications.

1 Motivation

The vast majority of evaluated nuclear data files present in state-of-the-art libraries, including the most recent ENDF/B-VII library [1], still lack information on the uncertainties associated with the evaluated physical quantities. This situation stems from the intrinsic difficulty in assessing those uncertainties (e.g., model errors), and from the lack of a strong incentive to provide them in the first place. Those two obstacles were lifted in recent years: the tremendous power of modern computers alleviated the first obstacle by providing means to sample the space around the evaluated data central values; and the recent surge in interest in innovative nuclear designs is pushing for the use of the evaluated libraries as predictive tools, beyond the traditional applications where numerous integral data were able to guide the evaluators work.

In this paper, we present our recent efforts to evaluate the covariance matrices for three major actinides, namely $^{235,238}\text{U}$ and ^{239}Pu , in the fast energy region. Next section is devoted to the presentation of the methodology used to assess uncertainties. A subset of all results is then discussed, along with the processing of the evaluated covariance matrices into multi-groups for use in applications. Finally, we discuss the present status of uncertainty evaluation for ENDF/B-VII, and some possible extensions and improvements upon this work.

2 Methodology

The evaluation of nuclear reaction data relies both on the statistical analysis of experimental data and on nuclear model calculations. When available, accurate experimental data are of great importance to guide theoretical calculations and constrain the model input parameters. However, experimental data sets are often limited to a particular reaction or/and energy domain, while an evaluation must cover a complete set of reactions occurring for a particular target nucleus and projectile, and this over a large incident energy range. Hence, nuclear model calculations fill the gaps by applying the constrained physical models to unexplored territories.

An approach to assess the uncertainties of the evaluated nuclear data should also reflect the evaluation methodology, and take into account uncertainties stemming from both experiment and theory. The methodology used here can be summarized as follows:

1. *Collect and analyze (i.e., evaluate covariance matrices of) all experimental data available.*

This is by far the most time consuming and difficult step, since it may involve the careful study of large sets of experimental data and the conditions in which they have been obtained. This is also the step where subjectivity or “expert guess” come (necessarily) into play.

2. *Evaluate a global experimental covariance matrix using a generalized least squares (GLS) technique or Bayesian method.*

Also this step is relatively straightforward from a mathematical point of view. Important questions can arise here (e.g., Peelle's Pertinent Puzzle, systematic vs. statistical errors, etc.).

3. *Perform nuclear reaction calculations, and obtain the sensitivity coefficients to the model input parameters.*

This is done by varying the model input parameters around their central values, and studying the influence of those variations on the calculated cross sections. It is assumed that the response is linear, and that non-linear effects are of second-order only. This assumption was checked in our calculations for all relevant parameters. Note that the central values of the model parameters were chosen according to the recent evaluation work on uranium isotopes by Young et al. [2].

4. *Combine experimental and model covariance matrices by applying a Kalman filter.*

A Kalman filter is nothing else than an automated Bayesian updating scheme to find the optimal set of parameters for a model calculation describing a set of experimental data [3]. In other words, the KALMAN code (by T. Kawano) that implements the Kalman filter, combines the information on experimental data and their

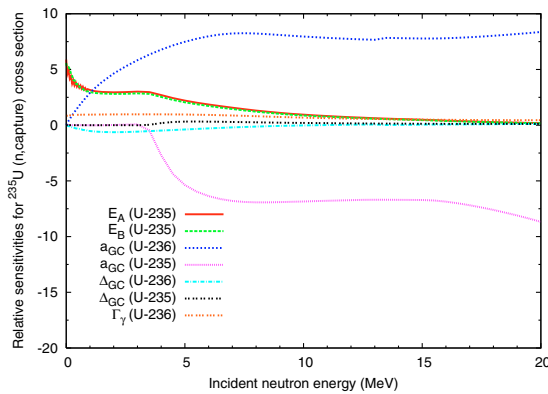


Fig. 1. Relative sensitivity coefficients for selected model parameters in the calculated ^{235}U (n,γ) cross section.

uncertainties, and the sensitivity of calculated cross sections to the model input parameters, and gives in output the optimal set of model parameters that best describe the experimental data.

5. *Process the evaluated point-wise covariance matrix into a multi-group covariance matrix.*

This step is done with the help of the processing codes NJOY [4] and ERRORJ [5].

3 Results

Due to the lack of space, we will focus (mostly) on the results obtained for $n+^{235}\text{U}$ reactions, since the exact same approach was used for the evaluation $n+^{238}\text{U}$ and $n+^{239}\text{Pu}$ reactions uncertainties. A detailed discussion of those results will be given in a separate, lengthened, publication.

3.1 Sensitivity calculations

Sensitivity calculations were performed by varying selected model input parameters in the ECIS03 [6] and GNASH [7] codes. Only the most relevant parameters were taken into account in the final evaluation. An example of sensitivity calculations results is shown in figure 1 in the calculation of the capture cross section of $n+^{235}\text{U}$. Relative sensitivities $\delta\sigma_i/\delta p_j$ are shown for the following parameters: fission barrier heights E_A and E_B in ^{235}U , level density parameters in the Gilbert-Cameron model (a, Δ) for $^{235,236}\text{U}$, and the absolute value of the gamma-ray strength function Γ_γ in ^{236}U .

At low incident neutron energies, the fission barrier heights have the most influence on the capture cross section. If the barrier heights are increased, the capture cross section is also increased (positive sensitivity coefficients) since the competing fission channel cross section is reduced. At higher energies, the most important parameters are the level density parameters a_{GC} in $^{235,236}\text{U}$, acting in opposite directions.

3.2 Optical model calculations and total cross section

Coupled-channels calculations were performed for all three isotopes, using the ECIS03 code [6] and optical potentials

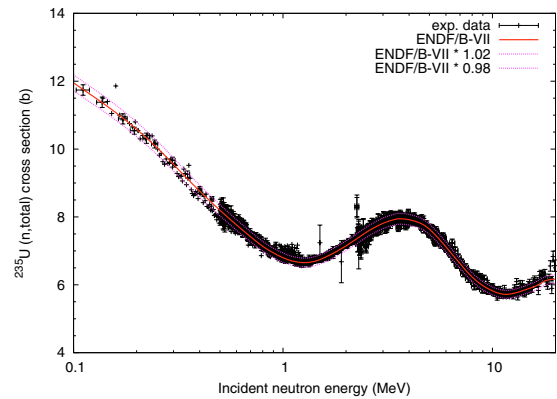


Fig. 2. Total cross section for $n+^{235}\text{U}$.

developed by P.G. Young [2] and recently included in the RIPL-3 database [8] with index numbers #3, #2006 and #7 for ^{235}U , ^{238}U and ^{239}Pu , respectively. Sensitivity calculations were performed by varying the following optical model parameters: the depth, radius and diffuseness for the real volume, imaginary volume, and real surface terms, and the (β_2, β_4) deformation parameters.

The calculated (n,total) cross section is shown in figure 2. Note that most experimental points lie in a $\pm 2\%$ uncertainty band, with incident neutron energies ranging from 30 keV up to 30 MeV. The calculated (n,total) cross section was slightly adjusted below 20 keV to better agree with experimental data. The evaluated covariance matrix for the total cross section is then used to constrain all other partial channels.

ECIS calculations also provided the transmission coefficients used in the Hauser-Feshbach equations for the emission probabilities of light particles from the excited compound nucleus.

3.3 Fission cross section

The neutron-induced fission cross section of ^{235}U was revisited recently by the IAEA/WPEC/CSEWG Standards group [9]. The ENDF/B-VII library incorporates the results of this group, including the covariance matrix obtained in the statistical analysis of all relevant experimental data. Since this is the most careful work done on this topic to date, we believe that it represents the best of our knowledge, both in terms of mean values, standard deviations and correlation coefficients.

The fission cross section is about 0.5–1.5% higher than the ENDF/B-VI.8 evaluation in the 1–5 MeV range, and 1–5% higher above 14 MeV, where new measurements from LAN-SCCE were made available.

Overall, the evaluated standard deviations are very small ($\leq 0.8\%$). The correlation matrix is shown in figure 3. It is worth noting that off-diagonal elements are almost zero, indicating very small *posterior* systematic errors.

3.4 Capture cross section

Direct measurements of the capture cross section of fissile nuclei are rare, difficult and subject to large errors, due to

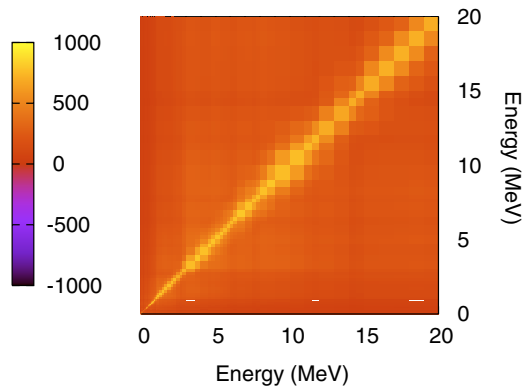


Fig. 3. Correlation matrix of the neutron-induced fission cross section of ²³⁵U, as evaluated by the IAEA/WPEC/CSWEG Standards group.

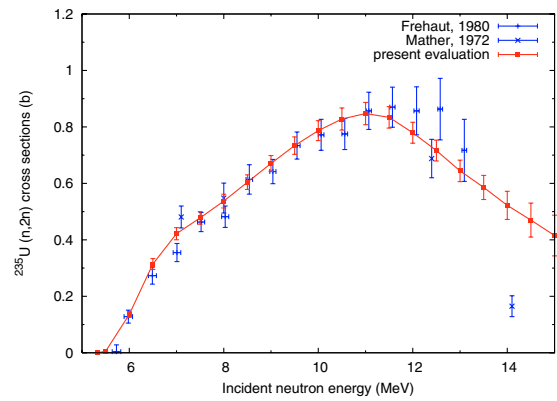


Fig. 5. Calculated ²³⁵U (n,2n) cross sections compared to existing experimental data.

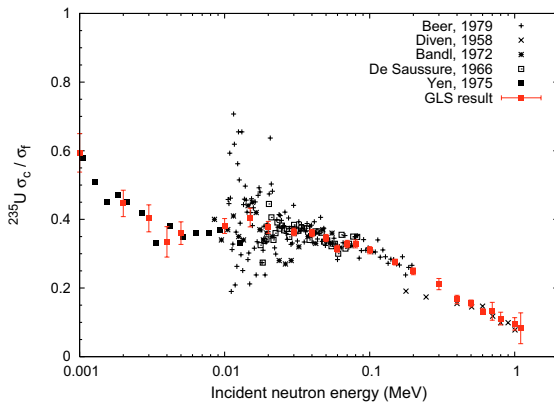


Fig. 4. Experimental measurements of the ratio $\alpha = \sigma_c/\sigma_f$ of $n+^{235}\text{U}$. The generalized least-squares solution (GLS) is shown in red.

the difficulties in distinguishing capture from fission events. More commonly, the ratio $\alpha = \sigma_c/\sigma_f$ of the capture to fission cross sections is assessed. Large discrepancies between existing α -measurements still remain. However, because the various experimental setups and procedures are different and mostly uncorrelated, uncertainties interfere incoherently in the generalized least-squares calculation, leading to a sizable reduction in the posterior uncertainties. The result is shown in figure 4.

3.5 Elastic and inelastic cross section

Elastic and inelastic scattering cross sections play an important role in determining the slowing down rate of neutrons in fast reactors. Unfortunately, their experimental study is hindered by energy resolution limits that in many cases prevent from resolving the elastic and first inelastic scattering groups. Our evaluation leads to uncertainties between 10 and 30% for incident neutron energies up to 20 MeV.

3.6 (n,xn) cross sections

At higher energies, (n,2n) and (n,3n) cross sections come into play. Only two experimental data sets are available, Fréhaut

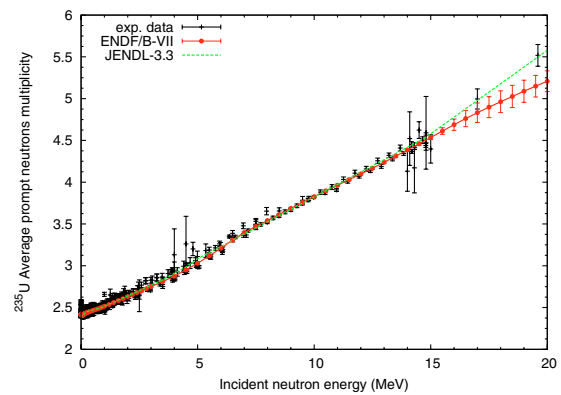


Fig. 6. Average prompt neutrons multiplicity for ²³⁵U.

(1980) and Mather (1972). GNASH results compare fairly with experimental data, as shown in figure 5. Beyond 14 MeV, uncertainties become large due to lack of experimental data.

3.7 Prompt neutrons multiplicity

The number of prompt neutrons emitted per fission event, or multiplicity, $\bar{\nu}_p$, is an important quantity both from theoretical (fission physics near the scission point) and applied (neutron balance in a reactor) point of views.

A rather large set of experimental data is available for the major three actinides studied here. Hence evaluated data rely mostly on statistical analyses of experimental data rather than on theoretical predictions, which do require some experimental information in input. A covariance analysis was performed for each nucleus, and the results were eventually adjusted within the uncertainty limits to improve the agreement with integral data. This is the case for ²³⁹Pu for which data from the Jezebel spherical critical assembly were used to constrain the product $\bar{\nu}_p \times \sigma(n, f)$.

Note that in all cases, experimental data were renormalized to the latest standard values of $\bar{\nu}_p(^{252}\text{Cf})$.

The results for ²³⁵U $\bar{\nu}_p$ are shown in figure 6. Off-diagonal elements of the covariance matrix are relatively small and will not be shown here. Standard deviations are almost always under 1%, except above 15 MeV where fewer experimental

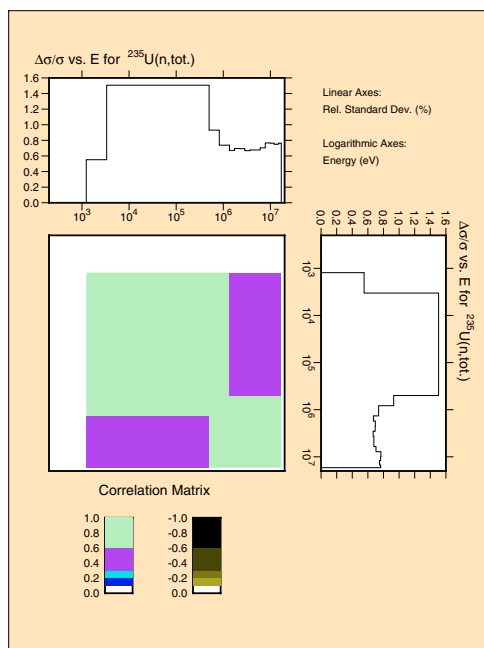


Fig. 7. Covariance matrix for the (n,total) cross section averaged in the ANL 15 energy group structure.

data are available. It also deviates from JENDL-3.3 values in this energy region.

4 Processing

Auxiliary utility codes were used to format the final results in ENDF format (MF31,33). The NJOY and ERRORJ processing codes were then used to produce grouped covariance matrices, in the 15-groups structure used at ANL for reactor sensitivity calculations (see Aliberti et al. in ref. [10]). A plot, generated by the NJOY code, of the energy-grouped covariance matrix for the (n,total) cross section is shown in figure 7.

5 Conclusion and future work

The ENDF/B-VII library represents a major step forward both in terms of quality and quantity of evaluations produced in a library. However very few covariance matrices i.e., evaluated uncertainty information, are included in the library as of today. No doubt the first revision of the library will address this issue.

The present work represents an effort to fill this gap and produce quality covariance matrices for a few isotopes of great importance. A companion effort was produced by Leal et al. at ORNL [11] to assess the uncertainties for the same isotopes and reactions in the resolved-resonance region. In addition,

D. Rochman et al. at BNL have worked on the evaluation of so-called “low fidelity” covariance matrices for a larger set of target nuclei [12].

Obviously, it is a first step, albeit important, and more remains to be done to produce increasingly reliable evaluated nuclear data and uncertainty data. Improvements over the existing methodology are currently under investigation in the OECD/WPEC Subgroup 24 led by M. Herman. The use of quality experimental information to constrain the evaluated covariance matrices is also evident, and several improvements to facilitate the access to this information would be valuable.

It is also important to note that the present uncertainty evaluation was done with the ENDF/B-VII evaluation itself, therefore lacking complete consistency. Future work will address this issue.

References

1. M.B. Chadwick, P. Oblozinsky, M. Herman et al., Nucl. Data Sheets **107**, 2931 (2006).
2. P.G. Young, M.B. Chadwick, R.E. MacFarlane, D.G. Madland, P. Möller, W.B. Wilson, P. Talou, T. Kawano, *Proceedings of the International Conference on Nuclear Data for Science and Technology, Santa Fe, 2004*, AIP Conf. Proc. **769** (2005), p. 290.
3. R.E. Kalman, Transaction of the ASME – Journal of Basic Engineering (1960), p. 35.
4. R.E. MacFarlane, Los Alamos National Laboratory Technical Report, LA-1274-M (1994).
5. G. Chiba, JNC TN 9520 2003-008 (2003).
6. J. Raynal, CEA Saclay, Report No. CEA-N-2772 (1994).
7. *Comprehensive Nuclear Model Calculations: Theory and Use of the GNASH Code*, P.G. Young, E.D. Arthur, M.B. Chadwick. *Proceedings of the IAEA Workshop on Nuclear Reaction Data and Nuclear Reactors: Physics, Design and Safety, Trieste, Italy, April 15–May 17, 1996* (World Scientific Publishing, Ltd., Singapore), Eds. A. Gandini, G. Reffo, (1998), pp. 227–404.
8. T. Belgia, O. Bersillon, R. Capote, T. Fukahori, G. Zhigang, S. Goriely, M. Herman, A.V. Ignatyuk, S. Kailas, A. Koning, P. Oblozhinsky, V. Plujko, P.G. Young IAEA-TECDOC-1506, IAEA, Vienna, 2005, Available online at <http://www-nds.iaea.org/RIPL-2/>.
9. V.G. Pronyaev, S.A. Badikov, A.D. Carlson, Z. Chen, E.V. Gai, G.M. Hale, F.-J. Hamsch, H.M. Hofmann, N.M. Larson, D.L. Smith, S.-Y. Oh, S. Tagesen, H. Vonach (to be published as an IAEA Technical Report).
10. G. Aliberti, G. Palmiotti, M. Salvatores, T.K. Kim, T.A. Taiwo, M. Anitescu, I. Kodeli, E. Sartori, J.C. Bosq, J. Tommasi, Ann. Nucl. Energy **33**, 700 (2006).
11. L.C. Leal, H. Derrien, N. Larson, G. Arbanas, R. Sayer, to be presented at the *International Conference on Nuclear Criticality Safety, St. Petersburg, Russia, May 2007*.
12. D. Rochman, M. Herman, P. Oblozinsky, S.F. Mughabghab, Report to the WPEC Subgroup 26 (2007).